JOURNAL OF OPTOELECTRONICS AND ADVANCED MATERIALS Vol. 12, No. 4, April 2010, p. 844 - 853

# Structural characterization of $Cu_{50}Zr_{50-x}Gd_x$ metallic glasses (x = 5, 10, 15, 20, 25) using Scanning Electron Microscopy

I.-V. STASI[a,b*], C. GHEORGHIEŞ[a], M.-I. URSU[b,c]
[a]*Faculty of Mechanical Engineering, "Dunarea de Jos" University of Galati, Domneasca Street, No.47, 800008, Romania*
[b]*S.C. Automobile DACIA S.A.,DIMat-R, Mioveni, Arges,Uzinei Street, No.1-3, 115400, Romania*
[c]*Faculty of Mechanical Engineering, "Gheorghe Asachi" Technical University of Iaşi, Bd. Dimitrie Mangeron, No. 61-63, 700050, Romania*

There is reported on a new class of a binary alloy composition capable of forming bulk metallic glasses based on the Cu-Zr system. The ternary $Cu_{50}Zr_{50-x}Gd_x$ alloys were prepared by Arc Melting of the pure elements to obtain the desired alloy composition. From Cu-Zr-Gd prealloys were prepared amorphous ribbons by Melt Spinning method. This work focuses on preparation of $Cu_{50}Zr_{50-x}Gd_x$ alloys and their characterization using scanning electron microscopy technique. The influence of gadolinium additions on structural behaviour of Cu-Zr system was studied. The precipitated phases obtained by SEM are identified by XRD techniques. The addition of gadolinium changes the crystallization behaviour of studied metallic glasses.

(Received April 7, 2010; accepted April 26, 2010)

*Keywords:* ternary $Cu_{50}Zr_{50-x}Gd_x$ metallic glasses, Melt Spinning, SEM

## 1. Introduction

Bulk metallic glasses (BMGs) have been largely investigated due to their unique physical, chemical and mechanical properties being of special interest for a wide range of potential applications. For the BMG-forming alloys, the number of components, the atomic size of the constituent elements, the composition and the cohesion between the metals are some of the crucial factors for the glass formation.

In this work the authors report on a new class of metallic glass in a simple Cu-base alloy. Recently, several metallic alloys were reported and extensive studies had been made in these glasses, such as Zr–Cu–Gd alloys. Very low critical cooling rates are required for these alloys to form metallic glasses, showing the possibility of producing bulk amorphous alloys by conventional casting processes. Without the limitation of size and shape, the amorphous alloys can be widely used as advanced materials [1].

In this paper the influence of gadolinium addition on structural and thermal behaviour of Cu-Zr bulk metallic glasses is studied.

## 2. Experimental procedures

The ternary $Cu_{50}Zr_{50-x}Gd_x$ alloys ingots were produced by Arc Melting using elements of high purity under argon atmosphere to obtain the desired alloy composition. For reaching homogeneity, the alloys were remelted several times. From Cu-Zr-Gd pre-alloys were prepared amorphous thin ribbons by Melt Spinning method under argon atmosphere (Fig. 1). Rapidly solidified and injection-cast specimens were prepared by re-melting the alloys in quartz tubes and ejecting with a specifical overpressure through a nozzle onto a cooper wheel rotating. The diameter of the copper roller is 30 cm, with the quenching temperature of 1300 K and the typical rotate speed of 65 Hz [2].

The macroscopically structures of $Cu_{50}Zr_{50-x}Gd_x$ alloys were studied in Light Room using a Gretag Macbeth SpectraLight III (at Daylight). The microscopically structures of the ribbons were investigated by using a Leica Microscope and a Quanta 200 SEM (Philips FEI Company). The amorphicity and crystalline phases of the specimen were examined by X-ray diffraction (XRD). The thermal property of the melt-spin ribbon was examined by using a Netzsch DSC404 system.

## 3. Results and discussion

Recently, a newest Cu-Zr binary equilibrium phase diagram has been given by Braga et al. through experiments, as can be seen in Ref. [3], which is quite different from the currently accepted one in some composition range. However, some discrepancies still exist as yet, so the equilibrium phase diagram of Cu-Zr

alloy used in this study is quoted from Ref. [4,5,6], as shown in Fig. 2 [1,2].

Fig. 3 shows the ternary equilibrium phase diagram of Cu-Zr-Gd.

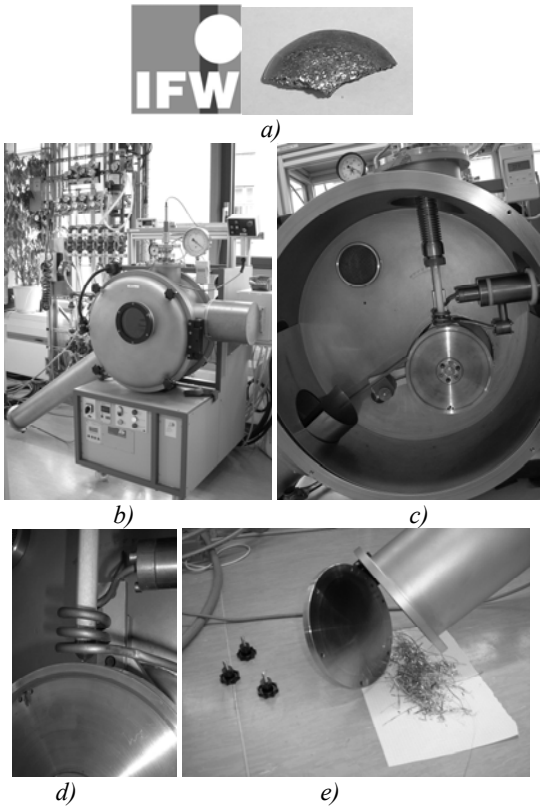


*Fig. 1. Preparation of $Cu_{50}Zr_{50-x}Gd_x$ ribbons by Melt Spinning: a) master alloy, b-c) Melt Spinner, d) The quartz tube for the master alloys, e) Preparation of $Cu_{50}Zr_{50-x}Gd_x$ ribbons.*

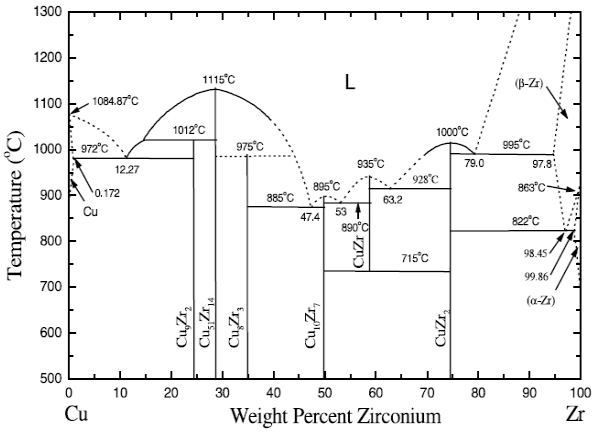


*Fig. 2. The equilibrium phase diagram of Cu-Zr*

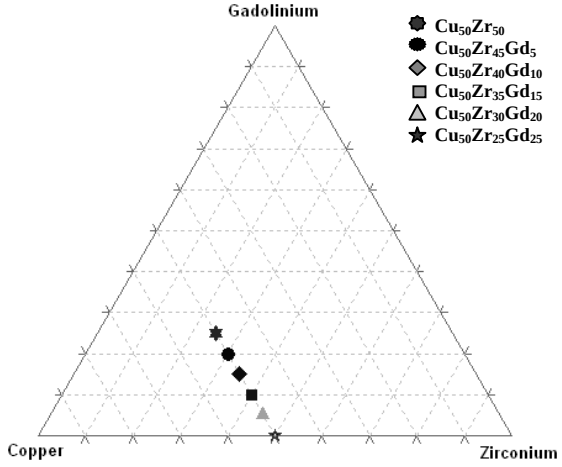


*Fig. 3. The ternary equilibrium phase diagram of Cu-Zr-Gd*

Fig. 4 shows the schematic diagram of crystallization process for amorphous $Cu_{50}Zr_{50-x}Gd_x$ alloys under the condition of continuous heating [1,2,6].

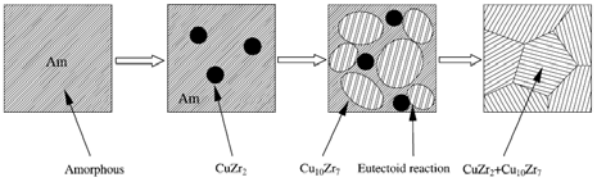


*Fig. 4. Schematic diagram of crystallization process for amorphous $Cu_{50}Zr_{50-x}Gd_x$ alloys [6]*

At room temperature Cu-Zr alloy matrix is fully amorphous, which can be confirmed from XRD pattern and TEM image of it. With increasing the temperature, relaxation process takes place and $CuZr_2$ phase begins to form from the amorphous matrix due to its large negative mixture enthalpy. At this stage, no $Cu_{10}Zr_7$ phase is detected just because an incubation time is required for it to precipitate and $CuZr_2$ phase starts to grow. After that, $Cu_{10}Zr_7$ phase precipitates a lot and its amount is larger than $CuZr_2$ phase.

In the subsequent stage, a eutectoid reaction occurs, that is, $Cu_{10}Zr_7 + CuZr_2 \leftrightarrow CuZr$ accompanying with the absorption of thermal. It is the eutectoid reaction that causes the appearance of the second endothermic peak in the DSC traces of amorphous Cu-Zr alloy. Attributing to the good lattice matching between $Cu_{10}Zr_7$ and $CuZr_2$ phases and that some $Cu_{10}Zr_7$ phases will probably take $CuZr_2$ particles as their nuclei, which decreases the free energy of nucleation and facilitates the crystallization process. Besides, a large amount of $Cu_{10}Zr_7$ phase is formed directly from the matrix, which retards the grain growth of $CuZr_2$ phase. As a result, the whole matrix is occupied by $Cu_{10}Zr_7$ phase in addition with part $CuZr_2$ one which consists of the main final crystallization products.

As for the CuZr phase, it can be neglected because of it small amount.

In summary, the crystallization process of amorphous Cu-Zr alloy with continuous heating can be expressed as follows [6]:

Fully amorphous → $CuZr_2$ particles + amorphous → $Cu_{10}Zr_7$ + $CuZr_2$ → $Cu_{10}Zr_7$ + $CuZr_2$ + CuZr (formed through eutectoid reaction $Cu_{10}Zr_7$ + $CuZr_2$ ↔ CuZr, but its amount is very small).

Due to the difference in chemical composition, the mean electron density varies locally, which can be detected by small-angle X-ray scattering (SAXS). The corresponding measurements will be performing at JUSIFA beam line at HASYLAB DESY Hamburg using X-ray energies.

Fig. 4 shows the important image of the rapidly quenched $Cu_{50}Zr_{50-x}Gd_x$ alloy. This typically images can be identified from macroscopically and microscopically analyses, as shown in Fig. 6-19.

The macroscopically analyses for $Cu_{50}Zr_{50-x}Gd_x$ alloys was done to identify the colours of the samples after two years after the samples were prepared by Melt Spinning (Fig. 5.). All samples were investigated in Light Room using a Gretag Macbeth SpectraLight III (at Daylight). The data are summarised in Table 1. for both side (glossy and frosted).

The microscopically analyses for all six samples for both sides were done using a Leica Microscope. The obtained images demonstrated one more time the same colour that was identified through macroscopically analyse using GretagMacbeth SpectraLight III, as shown in Fig. 6-17.

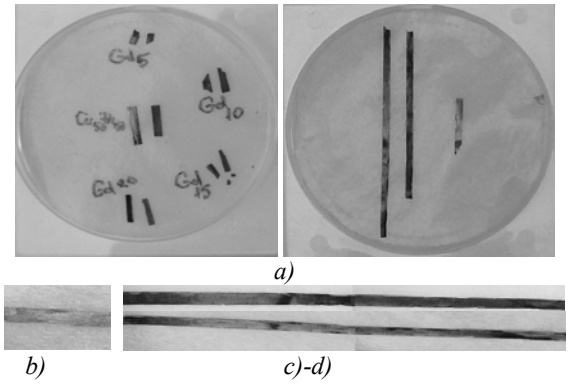


*Fig. 5. The macroscopically analyses for $Cu_{50}Zr_{50-x}Gd_x$ alloys: a) General view of $Cu_{50}Zr_{50-x}Gd_x$ (x=0,5,10,15,20) alloys, b) General view of $Cu_{50}Zr_{25}Gd_{25}$ alloy (frosted side of the ribbon), c-d) Detailed view $Cu_{50}Zr_{25}Gd_{25}$ alloy (glossy side of the ribbon)*

The ribbons were investigated and by using scanning electron microscopy (SEM) with a Quanta 200 SEM (Philips FEI Company). SEM images demonstrated that the microstructural evolution depends on the amount of gadolinium, as shown in Fig. 18.

Some important parts from every side of the sample are presented to characterized better the type of the ribbons. From that detailed images same phases can be identified, as shown in Fig. 19. (e.g. $Cu_{10}Zr_7$ + $CuZr_2$). The specifically structures (as shown in the Fig. 19.) can be identified and in the Figs. 6,12,14,17.

*Table 1.The structure of $Cu_{50}Zr_{50-x}Gd_x$ bulk metallic glasses.*

| No. | Sample | The side of the sample | Results | Figures |
|---|---|---|---|---|
| 1. | $Cu_{50}Zr_{50}$ | glossy side | grey colour with violet iridescences red with a particular shine gloss | Fig. 6. |
| | | frosted side | light mat grey with violet iridescences to red<br>the appearance of frosted side is identical with the glossy side, but is possible to identify a difference of shine | Fig. 7. |
| 2. | $Cu_{50}Zr_{45}Gd_5$ | glossy side | grey with violet iridescences<br>the violet tempt has been preserved, but the grey is more evident compared with the glossy side of the $Cu_{50}Zr_{50}$ alloy | Fig. 8. |
| | | frosted side | mat grey with violet iridescences but the tempt colour was changed in dark, compared with the frosted side of $Cu_{50}Zr_{50}$ alloy | Fig. 9. |
| 3. | $Cu_{50}Zr_{40}Gd_{10}$ | glossy side | dark grey, only a few traces of violet can be identified | Fig. 10. |
| | | frosted side | dark mat grey, the colour darkened very much and it doesn't have that violet shade | Fig. 11. |
| 4. | $Cu_{50}Zr_{35}Gd_{15}$ | glossy side | grey with some significant changes<br>the glass intensity is decreasing<br>the violet colour disappears and a tempted of yellow can be identified<br>therefore this glossy side of this type of alloy presents a light grey colour with yellow tempt<br>the glossy side is frosting | Fig. 12. |
| | | frosted side | mat grey with an easily tempt of yellow | Fig. 13. |
| 5. | $Cu_{50}Zr_{30}Gd_{20}$ | glossy side | grey with yellow-carroty tempt<br>yellow becomes yellow-carroty (almost orange)<br>it can be observed that one shining of colour had appeared | Fig. 14. |
| | | frosted side | mat grey, but darker<br>this side remains matte but the colour's intensity decreasing to light grey<br>the yellow loses from its intensity | Fig. 15. |

| | | | | |
|---|---|---|---|---|
| 6. | $Cu_{50}Zr_{25}Gd_{25}$ | glossy side | there is one mixture of colours: blue – violet – brown – red – orange – yellow – green and again blue and violet<br>due to this fact the authors called this alloy "the multicolour alloy" | Fig. 17. |
| | | frosted side | light grey with red iridescences | Fig. 16. |

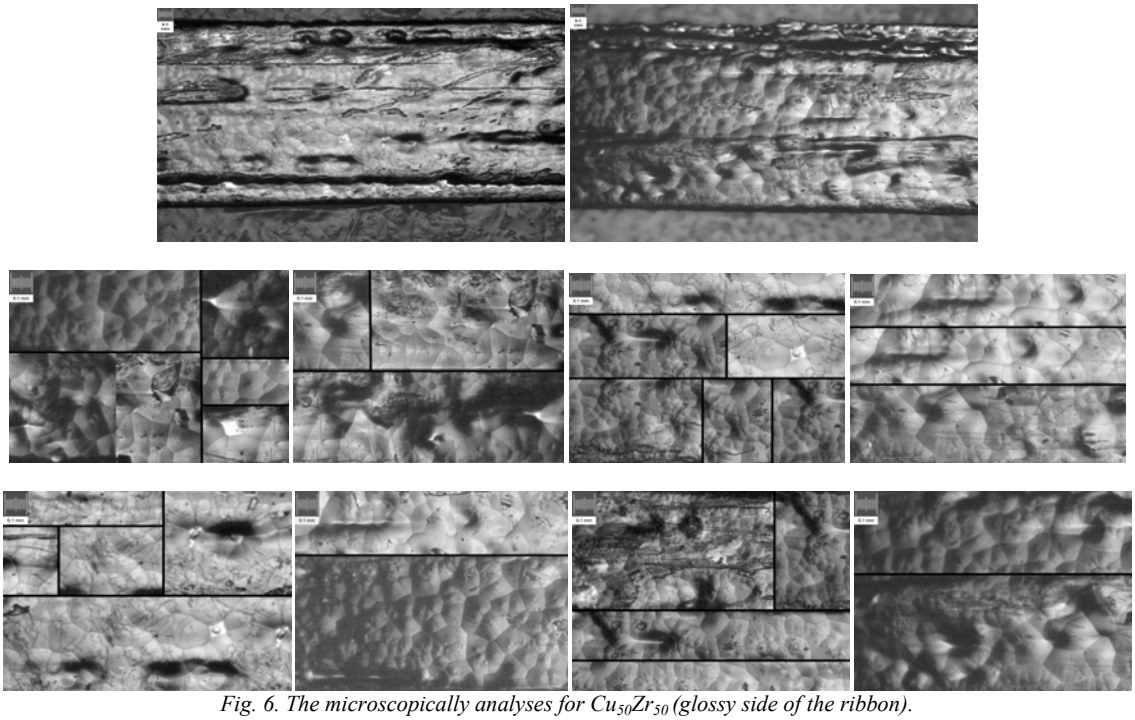

*Fig. 6. The microscopically analyses for $Cu_{50}Zr_{50}$ (glossy side of the ribbon).*

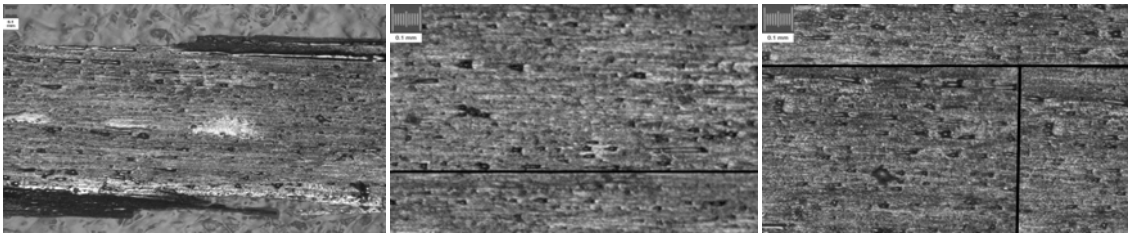

*Fig. 7. The microscopically analyses for $Cu_{50}Zr_{50}$ (frosted side of the ribbon).*

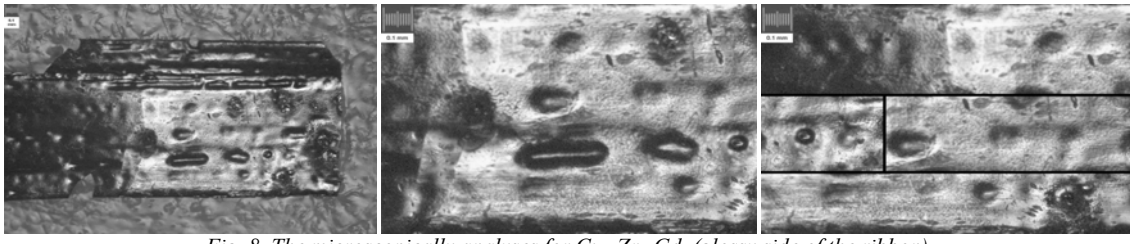

*Fig. 8. The microscopically analyses for $Cu_{50}Zr_{45}Gd_5$ (glossy side of the ribbon)*

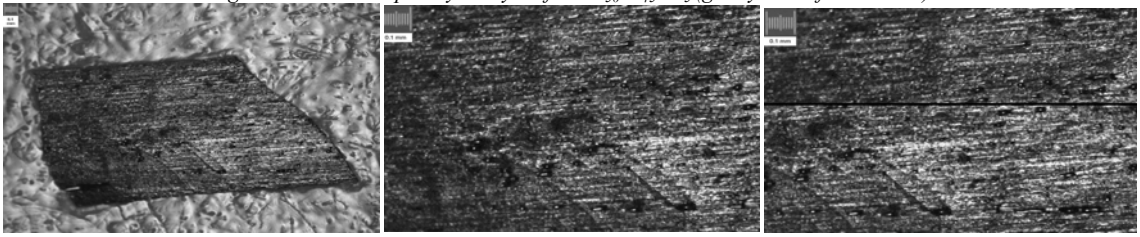

*Fig. 9. The microscopically analyses for $Cu_{50}Zr_{45}Gd_5$ (frosted side of the ribbon).*

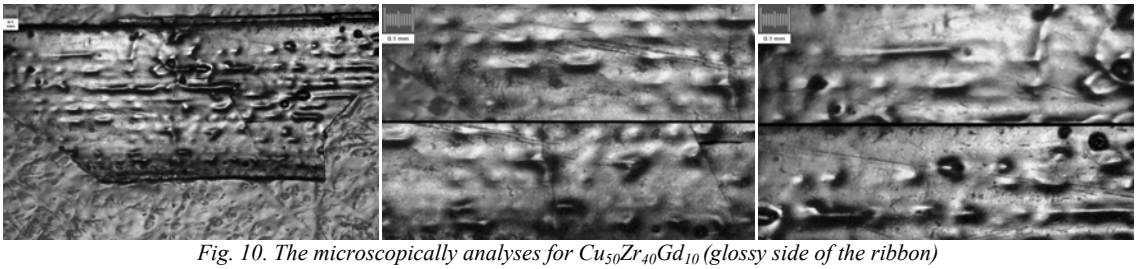

*Fig. 10. The microscopically analyses for $Cu_{50}Zr_{40}Gd_{10}$ (glossy side of the ribbon)*

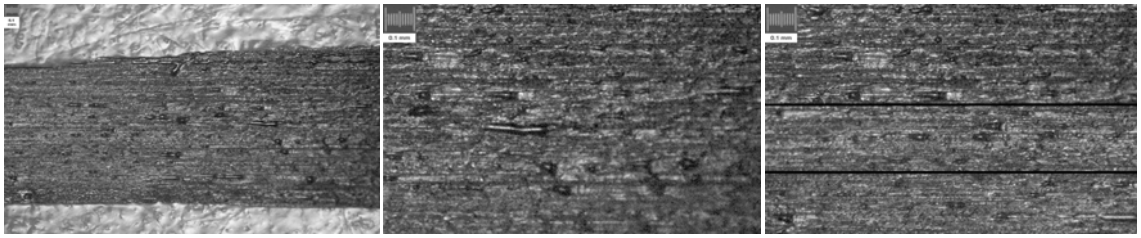

*Fig. 11. The microscopically analyses for $Cu_{50}Zr_{40}Gd_{10}$ (frosted side of the ribbon).*

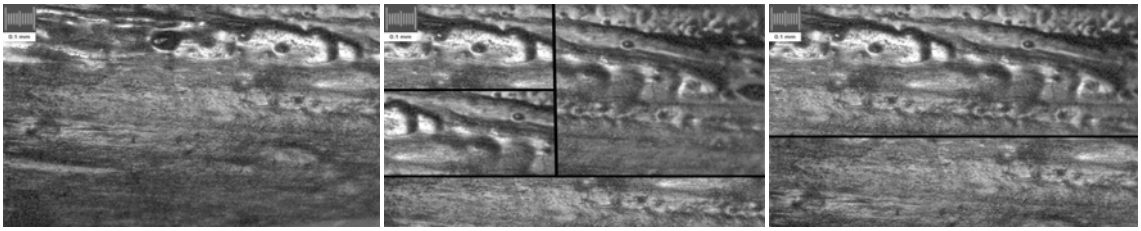

*Fig. 12. The microscopically analyses for $Cu_{50}Zr_{35}Gd_{15}$ (glossy side of the ribbon).*

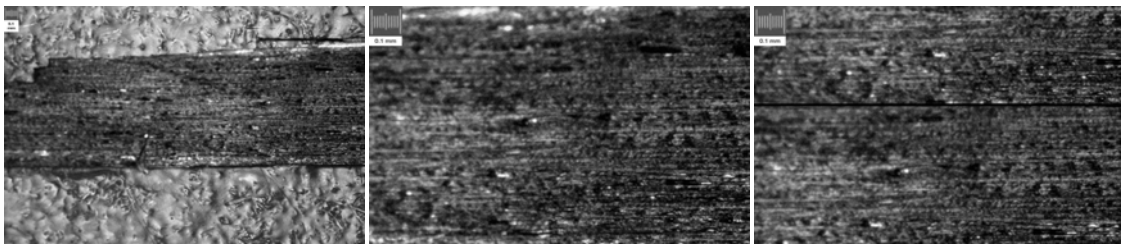

*Fig. 13. The microscopically analyses for $Cu_{50}Zr_{35}Gd_{15}$ (frosted side of the ribbon).*

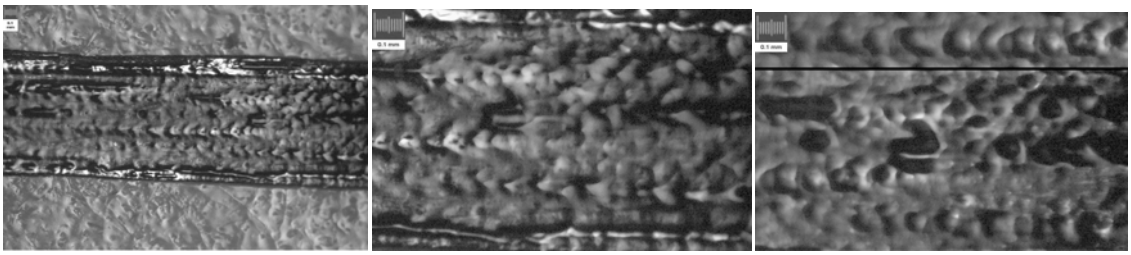

*Fig. 14. The microscopically analyses for $Cu_{50}Zr_{30}Gd_{20}$ (glossy side of the ribbon).*

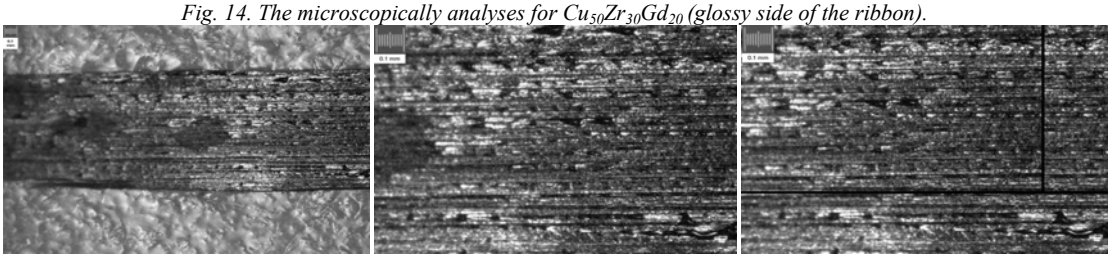

*Fig. 15. The microscopically analyses for $Cu_{50}Zr_{30}Gd_{20}$ (frosted side of the ribbon).*

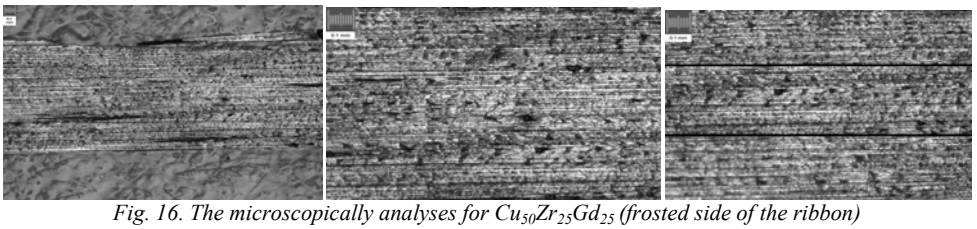

*Fig. 16. The microscopically analyses for $Cu_{50}Zr_{25}Gd_{25}$ (frosted side of the ribbon)*

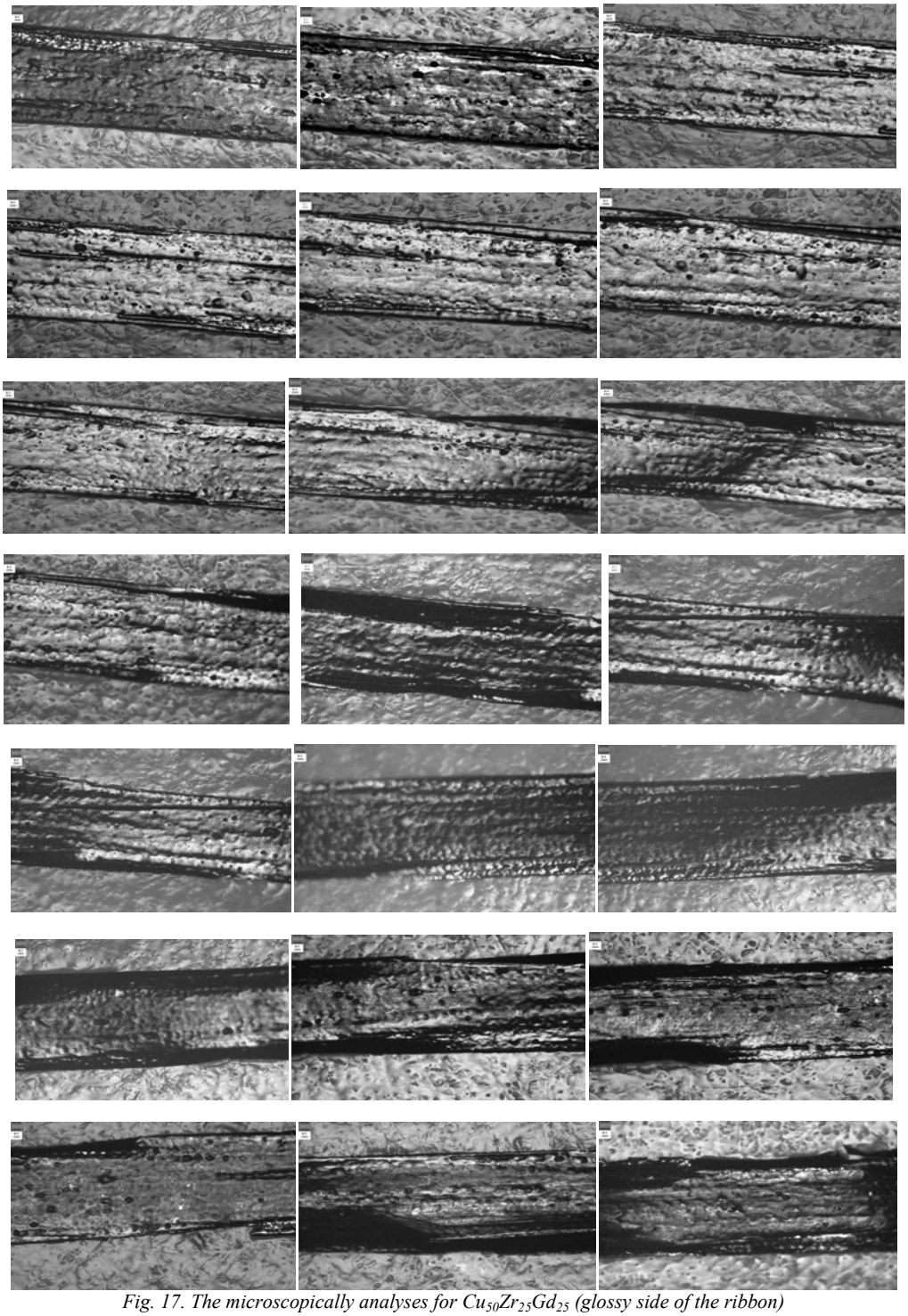

*Fig. 17. The microscopically analyses for $Cu_{50}Zr_{25}Gd_{25}$ (glossy side of the ribbon)*

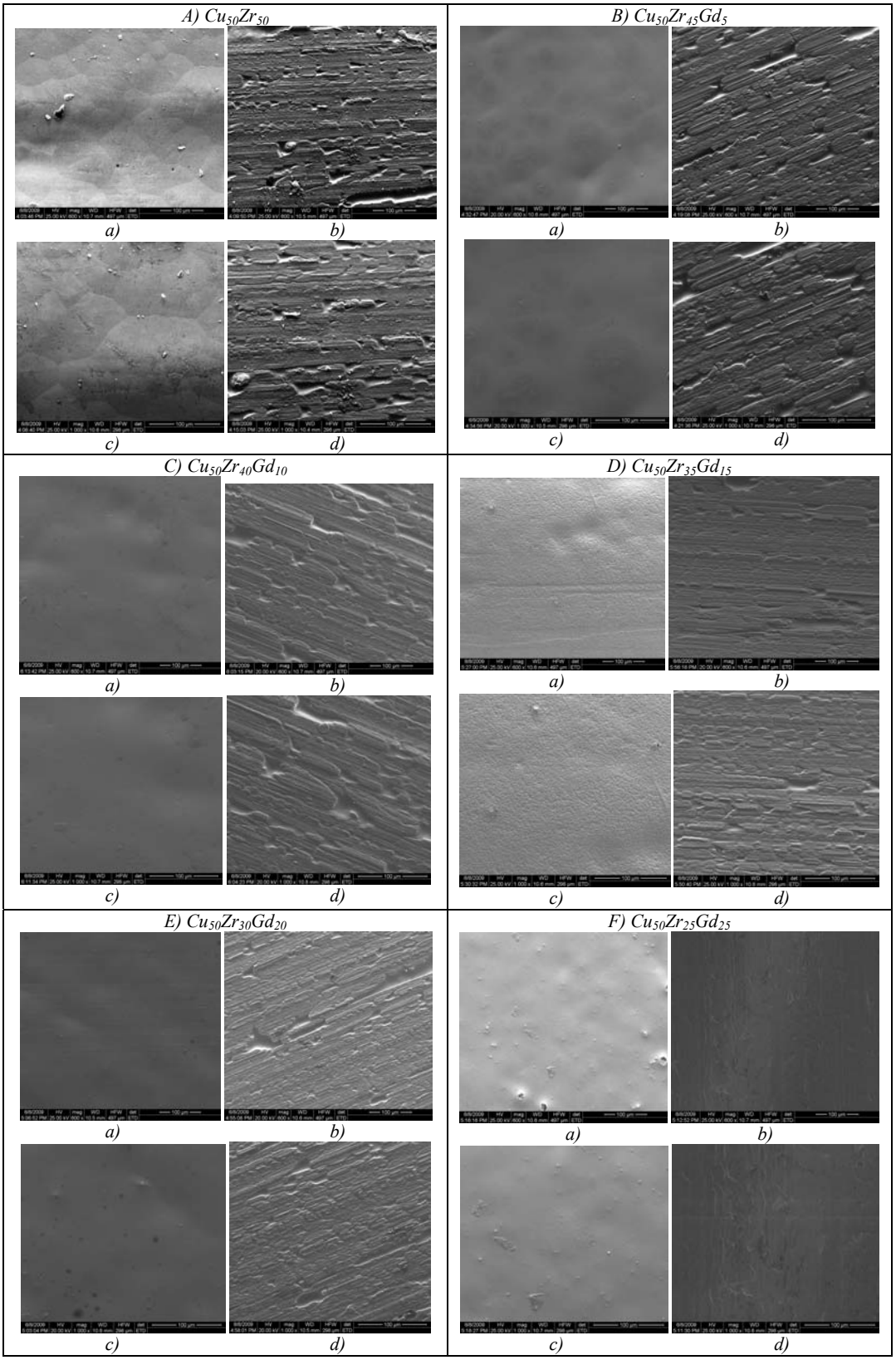


*Fig. 18. SEM images of $Cu_{50}Zr_{50-x}Gd_x$ alloys: a) Glossy Side - mag. 600 x, b) Frosted Side - mag. 600 x, c) Glossy Side - mag. 1000 x, d) Frosted Side - mag. 1000 x*

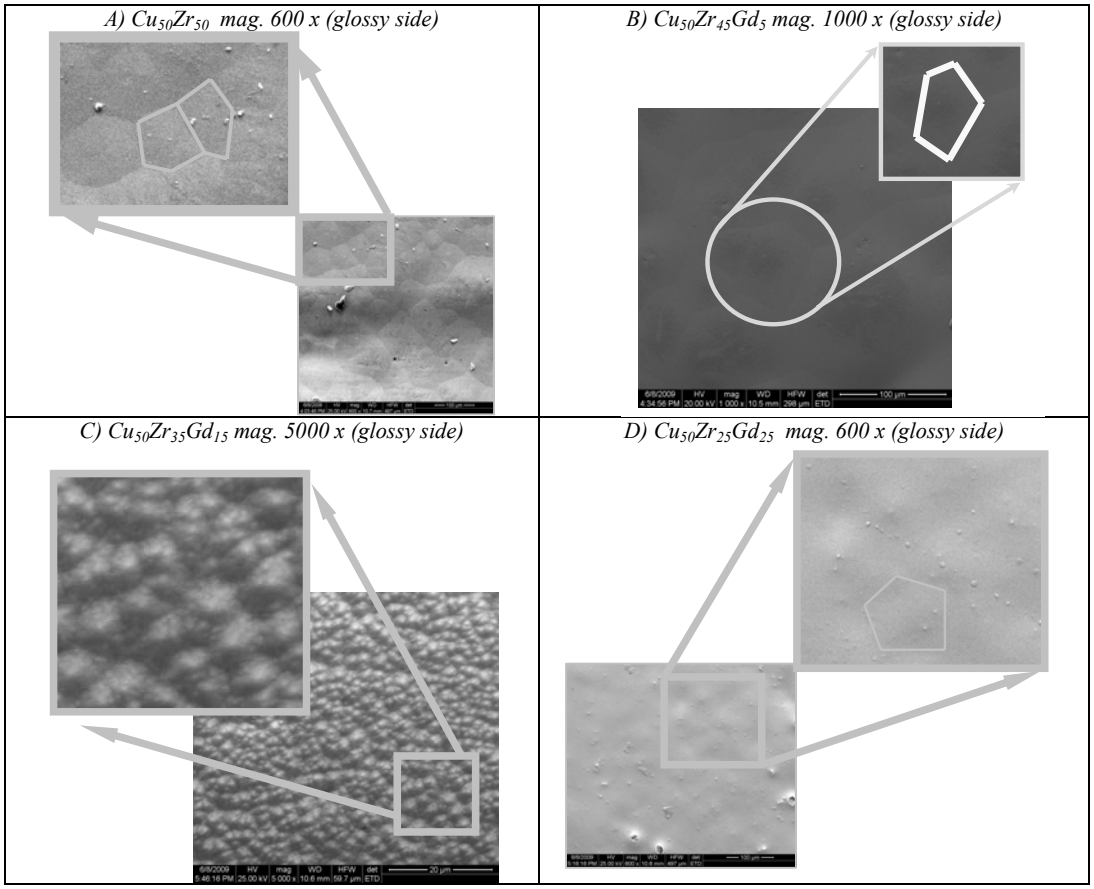


*Fig. 19. Detailed SEM images of $Cu_{50}Zr_{50-x}Gd_x$ alloys*

The structure of the ribbons was examined preliminarily by X-ray diffraction (XRD - Siemens D500 Diffractometer) using monochromatic Cu $K_\alpha$ radiation for 2θ range of 20-80°.

The XRD patterns of $Cu_{50}Zr_{50}$ show the identification of following important phases: $Cu_{10}Zr_7$, $CuZr_2$ and CuZr. The X-ray diffraction patterns of the investigated alloys are presented in Fig. 20. Almost all alloys show broad diffraction maxima characteristic for an amorphous structure. In a further work, this structural behaviour for $Cu_{50}Zr_{50-x}Gd_x$ will be discussed with more details based on complex XRD diffraction patterns.

The thermal stability of the alloys was examined with a differential scanning calorimeter (Netzsch DSC 404) under a flow of purified argon using a constant heating rate of 20 K/min. Thermal analysis of the ribbon samples was carried out to determine the glass transition temperature, $T_g$, and the crystallization onset temperature, $T_x$.

Fig. 21 compares the crystallization behaviour of the amorphous alloys $Cu_{50}Zr_{50-x}Gd_x$ by their DSC curves. The crystallization temperature of amorphous $Cu_{50}Zr_{50}$ decreases with gadolinium content and changes from a single step crystallization into two steps. The DSC traces of the $Cu_{50}Zr_{50-x}Gd_x$ alloys showing a glass transition followed by crystallization. For all alloys, the crystallization happens in well-separated steps, as can be seen in DSC traces. The DSC traces can be clearly classified into two groups based on the temperature range of the exothermic reactions (ERs), i.e. low-temperature ER with $T_x$ in the range of 200-230 °C (referred to as peak I) for the alloys x=20, 25; and high-temperature ER with $T_x$ in the range of 340-430 °C (referred to as peak II) for the alloys x=5,10,15,20,25. Interestingly, the wide composition range of $20 \leq x \leq 25$ showed two separated ERs related to peaks I and II.

The DSC results strongly suggest that phase separation occurred in rapidly solidified alloys with Gadolinium content above 20 at.%.

The characteristic values of the crystallization temperatures $T_x$ are summarized in Table 2.

DSC is one of the most frequently used techniques in the field of thermal characterization of solids. The method is used for the analysis of energetic effects such as: melting/crystallization behaviour, glass transition, solid-solid reactions, degree of crystallinity and specific heat. In a further work, this thermal behaviour for $Cu_{50}Zr_{50-x}Gd_x$ will be discussed with more details.

The atomic structures and the crystallization behaviour of amorphous alloys are significant to the understanding mechanism of plasticity in amorphous alloys because the activation energy for crystallization is related to the atomic arrangement of the amorphous structure. In general, the phase separation in the liquid state is believed to play an important role to the

crystallization process, which in turn can affect the plastic deformation.

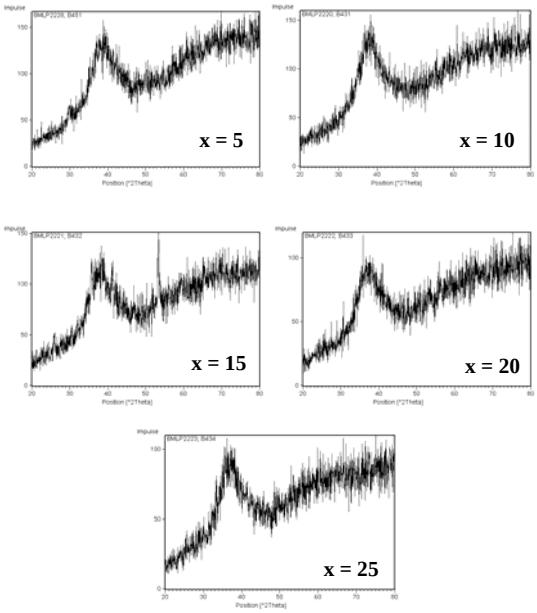


*Fig. 20. X-ray diffraction patterns (Cu $K_\alpha$ radiation) for $Cu_{50}Zr_{50-x}Gd_x$ ribbons*

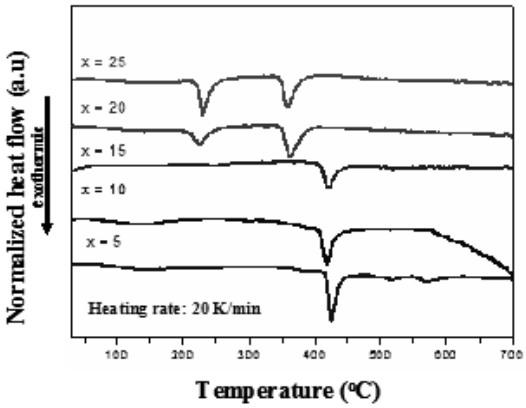


*Fig. 21. DSC traces obtained at 20 K/min for $Cu_{50}Zr_{50-x}Gd_x$ alloys*

*Table 2. The characteristic values of the crystallization temperatures.*

| No. | Alloy | $T_{x1}$ (°C) | $T_{x2}$ (°C) |
|---|---|---|---|
| 1 | $Cu_{50}Zr_{45}Gd_5$ | | 419 |
| 2 | $Cu_{50}Zr_{40}Gd_{10}$ | | 408.6 |
| 3 | $Cu_{50}Zr_{35}Gd_{15}$ | | 410 |
| 4 | $Cu_{50}Zr_{30}Gd_{20}$ | 213 | 352.6 |
| 5 | $Cu_{50}Zr_{25}Gd_{25}$ | 223.5 | 349.2 |

Besides, the investigation of the glassy nature of the alloys through XRD and DSC experiments, TEM studies were performed to reveal the details of structure at atomic resolution. Part of the specimen of $Cu_{50}Zr_{50-x}Gd_x$ alloy will be supplied for transmission electron microscopy (TEM) observation to check the microstructures for crystallized specimen with a Tecnai F30 Analytical Microscope (Philips FEI Company).

## 4. Conclusions

Nucleation studies of bulk metallic glasses are of great importance in understanding the mechanisms of phase transformation far from equilibrium, evaluating the glass-forming ability (GFA) of the melt and producing controlled microstructure.

To extend the application of structural bulk metallic glasses, it is important to combine high glass-forming ability and good mechanical properties. In the case of Cu-based bulk amorphous alloys, recent studies have found that the addition of Gd to the Cu-Zr binary system reduces the melting temperature, which strongly correlates with the good glass-forming ability. New Cu-based bulk amorphous alloys where formed in $Cu_{50}Zr_{50-x}Gd_x$ (x=5,10,15,20,25) ternary alloys by a single roller melt-spinning technique.

The structural and thermal behaviour of this type of BMGs was investigated in this paper. The addition of gadolinium changes the crystallization and thermal behaviour of $Cu_{50}Zr_{50}$ bulk metallic glasses. This addition greatly improves its glass-forming ability.

Cu-based BMGs have significant importance in basic research and engineering aspects.

Therefore, these types of BMGs are very promising for the further development of Cu-Zr-based alloys as advanced materials. Cu-based amorphous alloys have a potential for practical application due to their unique properties and relatively low material cost compared with commercial materials.

**Acknowledgements**

Special thanks are due Prof. Dr. Jurgen Eckert, Niculae Boicea, Prof. Mariana Calin and Dr. Norbert Mattern for their guidance and valuable help on each stage of the process.

The authors thank for technical assistance to: Angelica-Domnica Botezatu (SEM), Andrea Ostwaldt (XRD), Birgit Bartusch (DSC) and Donath Sven (Melt Spinning).

Financial support provided by European Union within the framework of the research and training networks of BMG: "Ductilisation of Bulk Metallic Glasses by Length-scale Control in BMGs Composites and Applications" (MRTN-CT-2003-504692).

The authors are grateful to the IFW Dresden and S.C. Automobile Dacia S.A. Mioveni (Department of Materials Engineering – DIMat-R) for them technical support.

## References

[1] I. V. Stasi, C. Gheorghieş, N. Mattern, J. Eckert, J. Optoelectron. Adv. Mater. **11**, 2963 (2008).
[2] I. V. Stasi, G. Nedelcu, C. Gheorghieş, N. Mattern, J. Eckert, J. Optoelectron. Adv. Mater. **12**, 3465 (2008).
[3] M. H. Braga, L. F. Malheiros, F. Castro, D. Soares, Z. Metallkd. **89**, 541 (1998).
[4] P. Villars, L.D. Calvert, in: Pearson's Handbook of Crystallographic Data for Intermetallic Phase, Materials Park Press, 1511 (1991).
[5] K. J. Zeng, M. Hämäläinen, H.L.Lukas: Phase diagram of Cu-Zr alloys, J. Phase Equilibria **15**, 577 (1994).
[6] H. R. Wang, Y. F. Ye, Z. Q. Shi, X. Y. Teng, G. H. Min, Journal of Non-Crystalline Solids **311**, 36 (2002).

*Corresponding author: vis13_2000@yahoo.com